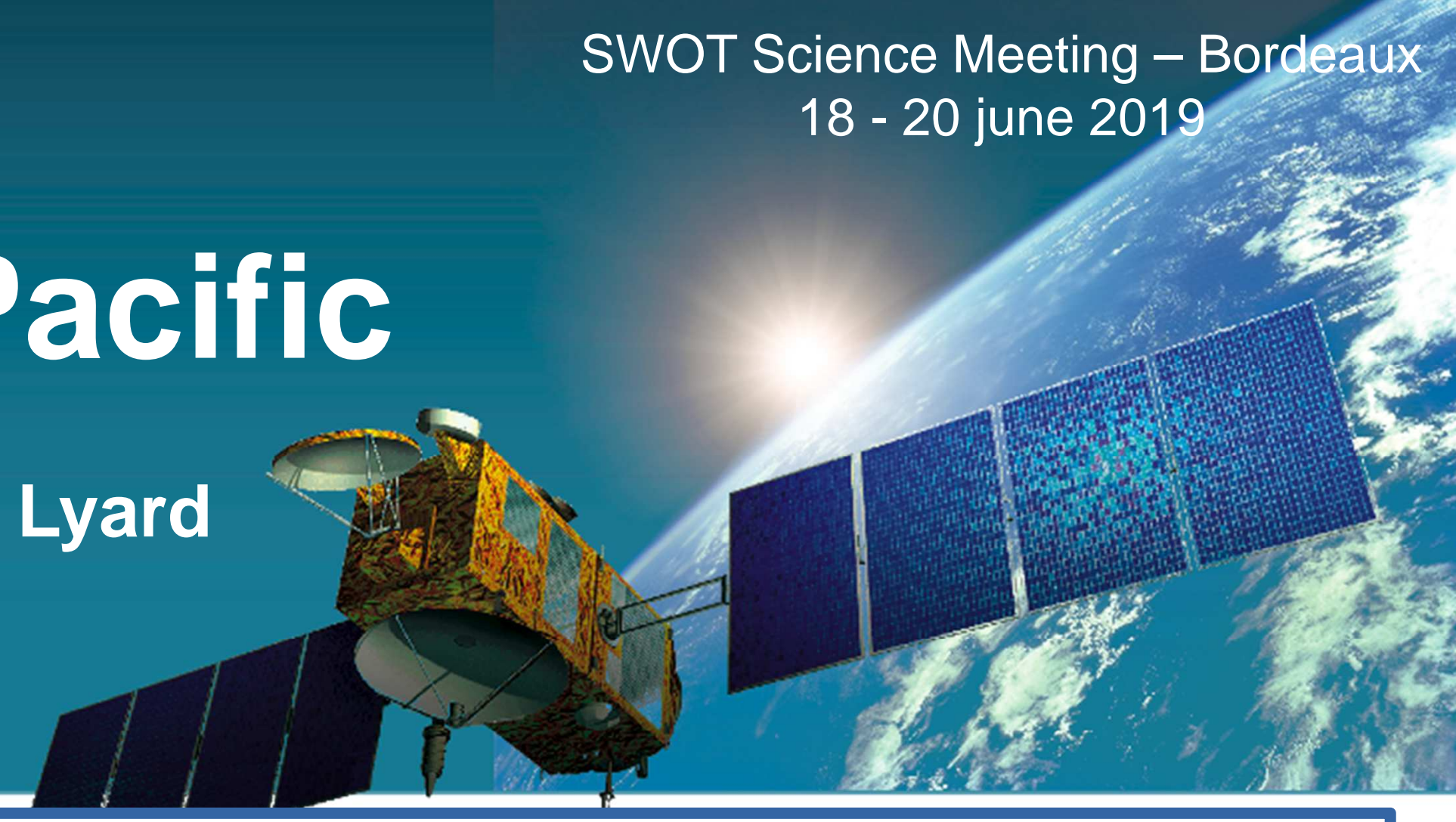




SWOT in the tropics: A case study in the South West Pacific

L. Gourdeau, F. Marin, M. Tchilibou, G. Sérazin, R. Morrow, F. Lyard

LEGOS, IRD/CNES/CNRS/UPS, Toulouse, France



1. Motivation

The tropical Pacific ocean is characterized by:

- strong zonal currents (Figs. 1.1) and a high EKE level.
- intense meso/submesoscale features (Fig. 2.1)
- a flatter SSH spectrum in the altimetry (Fig. 1.2) than in numerical models

The main goal of this project is to assess the observability of SWOT in the tropical Pacific Ocean, with a special focus on 2 regions of the SouthWest basin where mesoscale activity and internal tides are equally important :

- the **Solomon Sea** (major pathway between the Southern Pacific and the equatorial region, Tchilibou et al., 2018, 2019)
- **New Caledonia** (to prepare an *in situ* cal/val experiment during the 1-day SWOT orbit, Sérazin et al., 2019)

The specific objectives are to investigate the spatio-temporal dynamics of meso/submesoscales in the tropics, to give insight into their signature in sea level and to analyze their impact onto the large-scale ocean circulation.

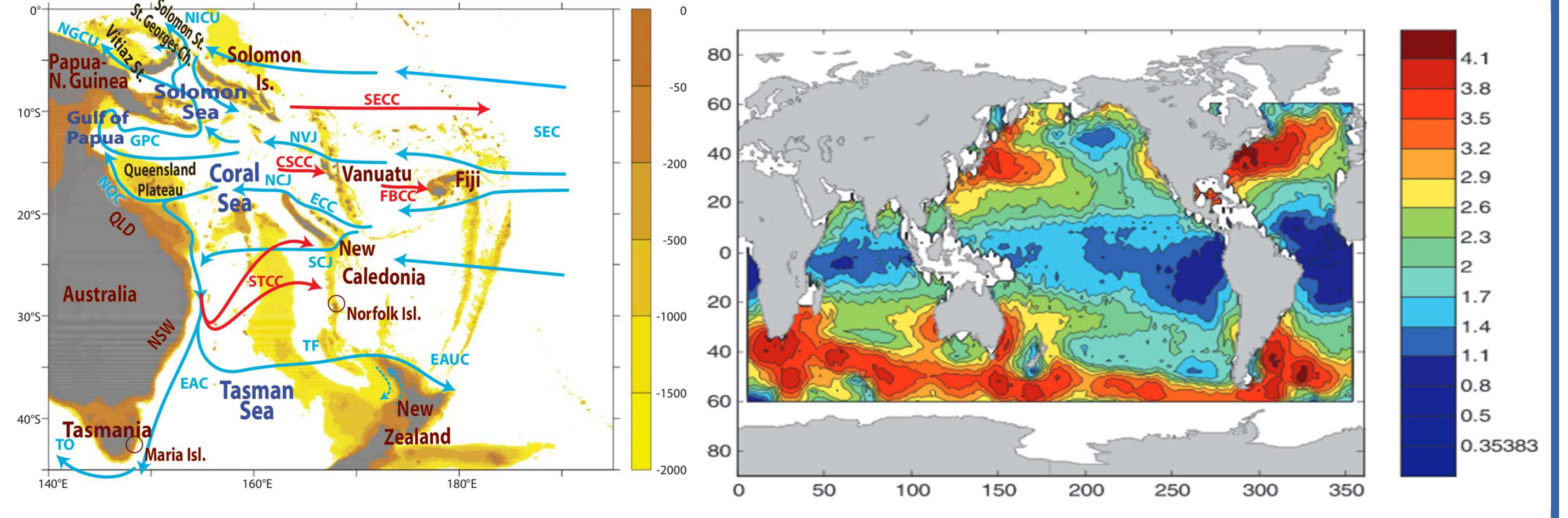


Fig. 1.1: Schematic ocean circulation in the SouthWest tropical Pacific (Ganachaud et al. 2014) : mean currents, integrated 0-1000m (blue arrows) and surface-trapped countercurrents (red arrow). Bathymetry in color.

Fig. 1.2: SSH spectral slopes in the 70-250 km band from altimetry (Xu and Fu, 2011)

2. Spectral signature of the Tropical Pacific Dynamics

Global DRAKKAR simulation (G12) – NEMO model, 1/12° resolution, 46 vertical levels, ERA-INTERIM forcing (1989-2007), 5-day outputs (Djath et al. 2014)

- large range of scales and strong anisotropy for mesoscale structures near the equator
- smaller-scale turbulent structures in off-equatorial region

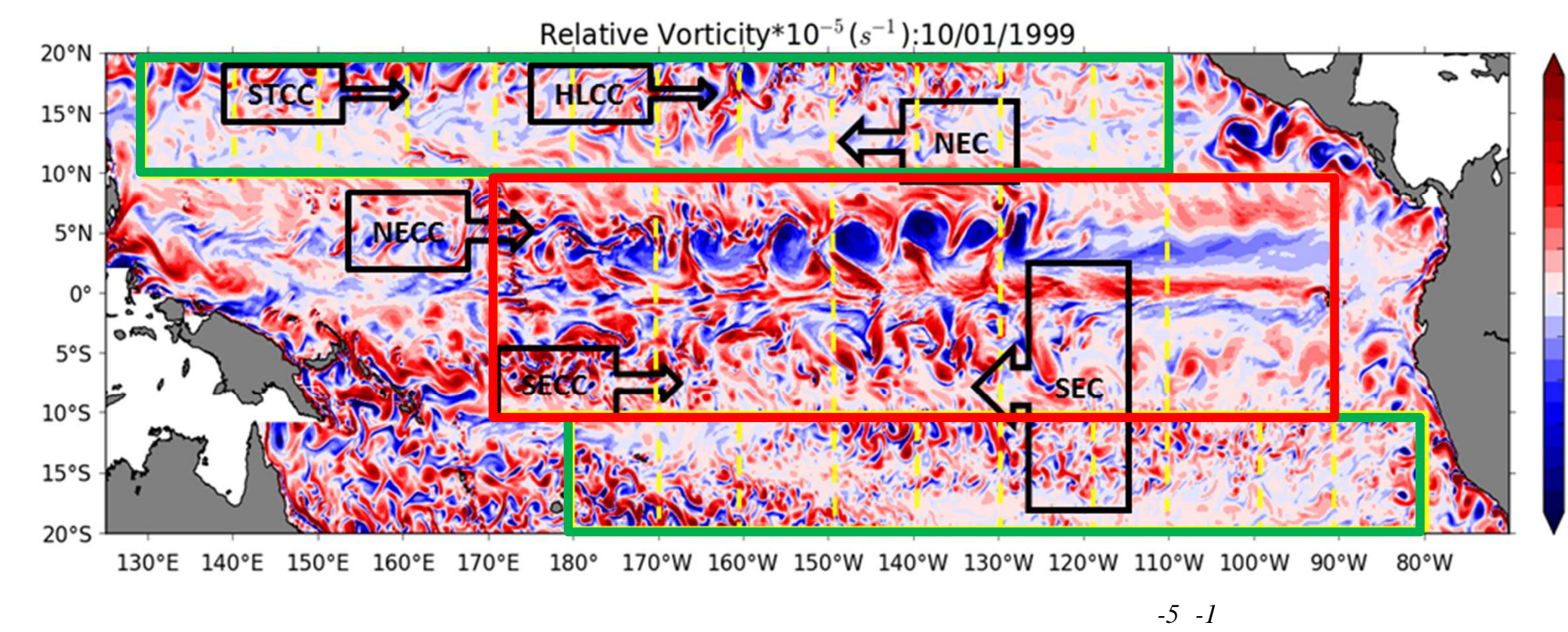


Fig. 2.1: Snapshot of relative vorticity in the G12 simulation (unit : $10^{-5} s^{-1}$). Yellow lines delineate the equatorial and off-equatorial region. Dashed lines delineate square boxes for the different regions to compute wavenumber spectra. Black arrow illustrate the main tropical surface currents.

Equatorial versus off equatorial dynamics

Off equator (10°N-20°N et 10°S-20°S): Mesoscale range: < 250 km
From isotropic turbulence to Rossby waves

Equator (10°S-10°N): Mesoscale range: < 800 km
Two distinct dynamical regimes:

- Long equatorial waves (zonal anisotropy)
- Tropical instability waves and equatorial « mesoscale » (Meridional anisotropy)

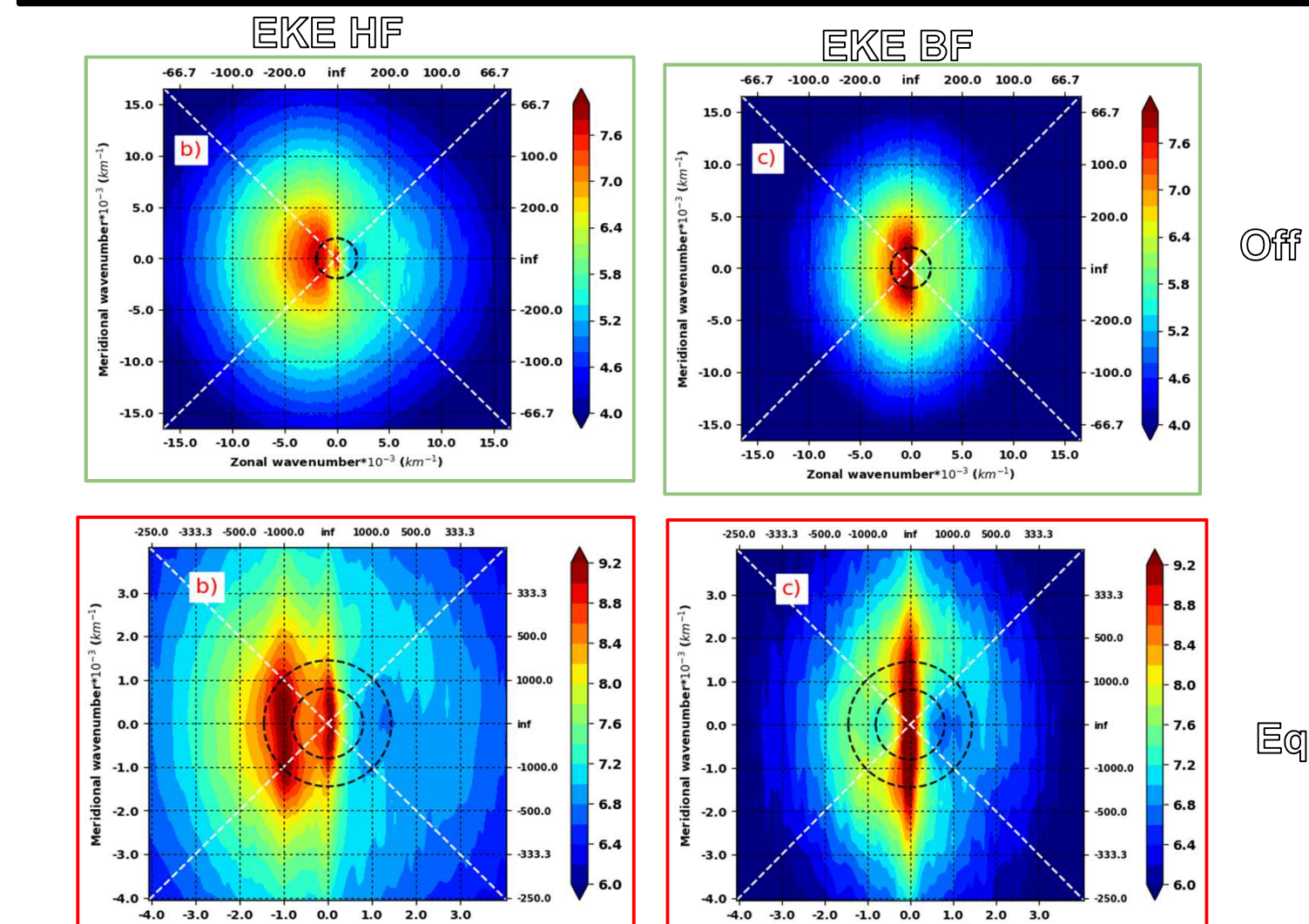


Fig. 2.2: Zonal-meridional wavenumber EKE spectra over 10°NS-20°N S (Off Eq) and 10°S-10°N (Eq) for high frequency motions (< 90 days, EKE HF) and low frequency motions (> 90days, RKS LF)

Comparison of SSH/EKE spectra in equatorial and off-equatorial regions

Equator: high EKE energy, low SSH variability → Agostrophic dynamic

SSH altimetric spectra distinguish from modelled spectra for $L < 300$ km
→ flatter spectra ($k^{-5} \rightarrow k^{-1}$) → higher variance → inertia gravity waves???

Internal tide signature:
No more discrepancy between modelled and altimetric spectra

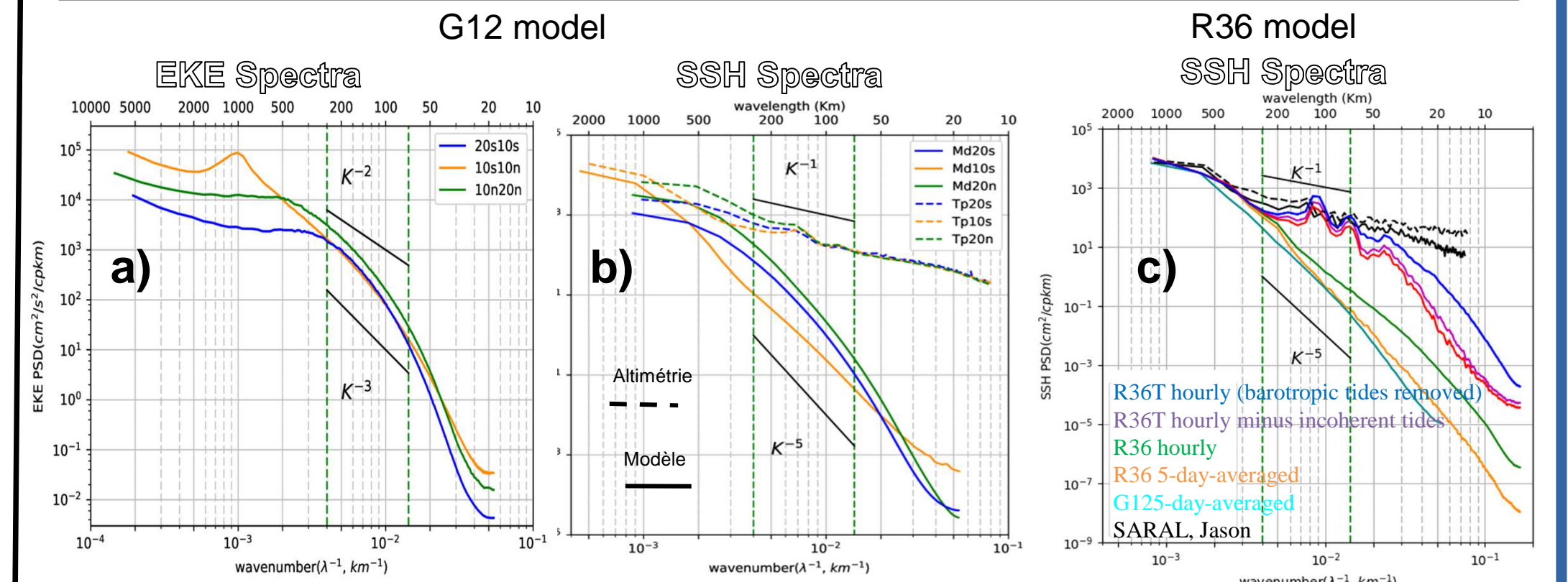


Fig. 2.4: a) EKE and b) SSH spectra over 20°S-10°S (blue), 10°S-10°N (orange) and 10°N-20°N (green) from G12 model (solid lines) and Topex-Poseidon (dashed lines). c) SSH spectra at 163° E between 2°S-13°S from R36 model including explicit tides (see below). Compared to the orange spectrum, the green spectrum gives evidence of internal waves, the red spectrum of M2 coherent baroclinic tide, the purple spectrum of the full coherent baroclinic tides, and the blue spectrum of the full signal once the barotropic tides has been removed.

3. M2 Internal tides in the Solomon Sea

Regional configuration of NEMO3.6 - 1/36°, 75 vertical levels, GEBCO08 bathymetry, interannual DFS5.2 forcing (1992-2000)

- 2 versions : without tides (R36) and with tides (R36T) / 9 tide constituents from FES2014: K1,O1,P1,Q1,M2,N2,S2,K2,Ms4
- 2 outputs : hourly (El Niño: Jan-Mar 1998; La Niña: April-June 1999) / daily (Jan 1998- Dec 1999)

→ projection on the 10 first vertical modes to separate barotropic and baroclinic tides

Validation

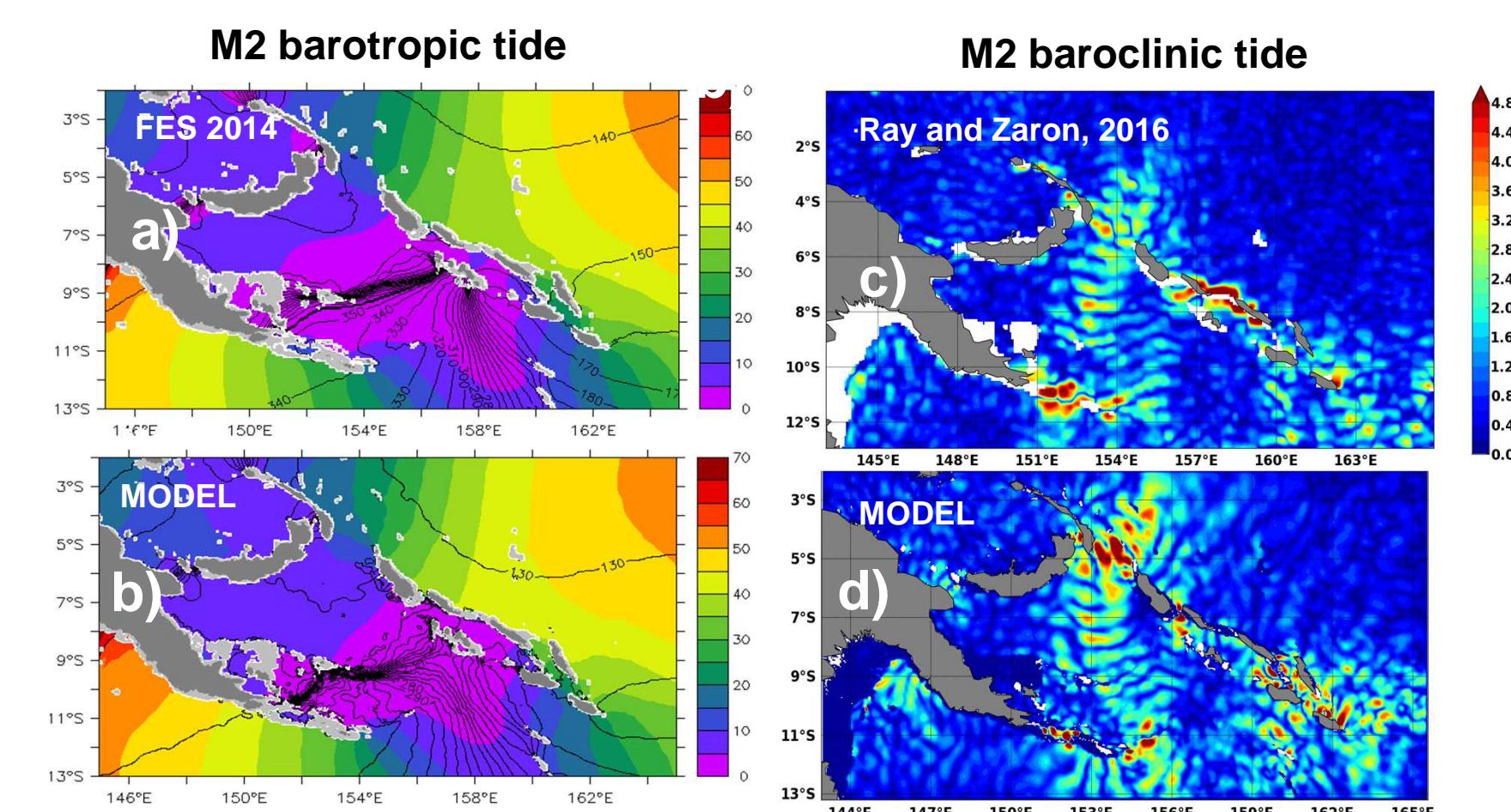


Fig. 3.1: M2 barotropic amplitude (cm) and phase (contours) from a) model and b) FES 2014 (Lyard et al. 2018). M2 baroclinic tides amplitude from c) Model and d) Ray and Zaron (2016) altimetric analyses.

M2 internal tides generation and propagation

- conversion of 14GW from barotropic to baroclinic tides
- 3 main sites of generation
- M2 kinetic energy confined to the first 300 meters

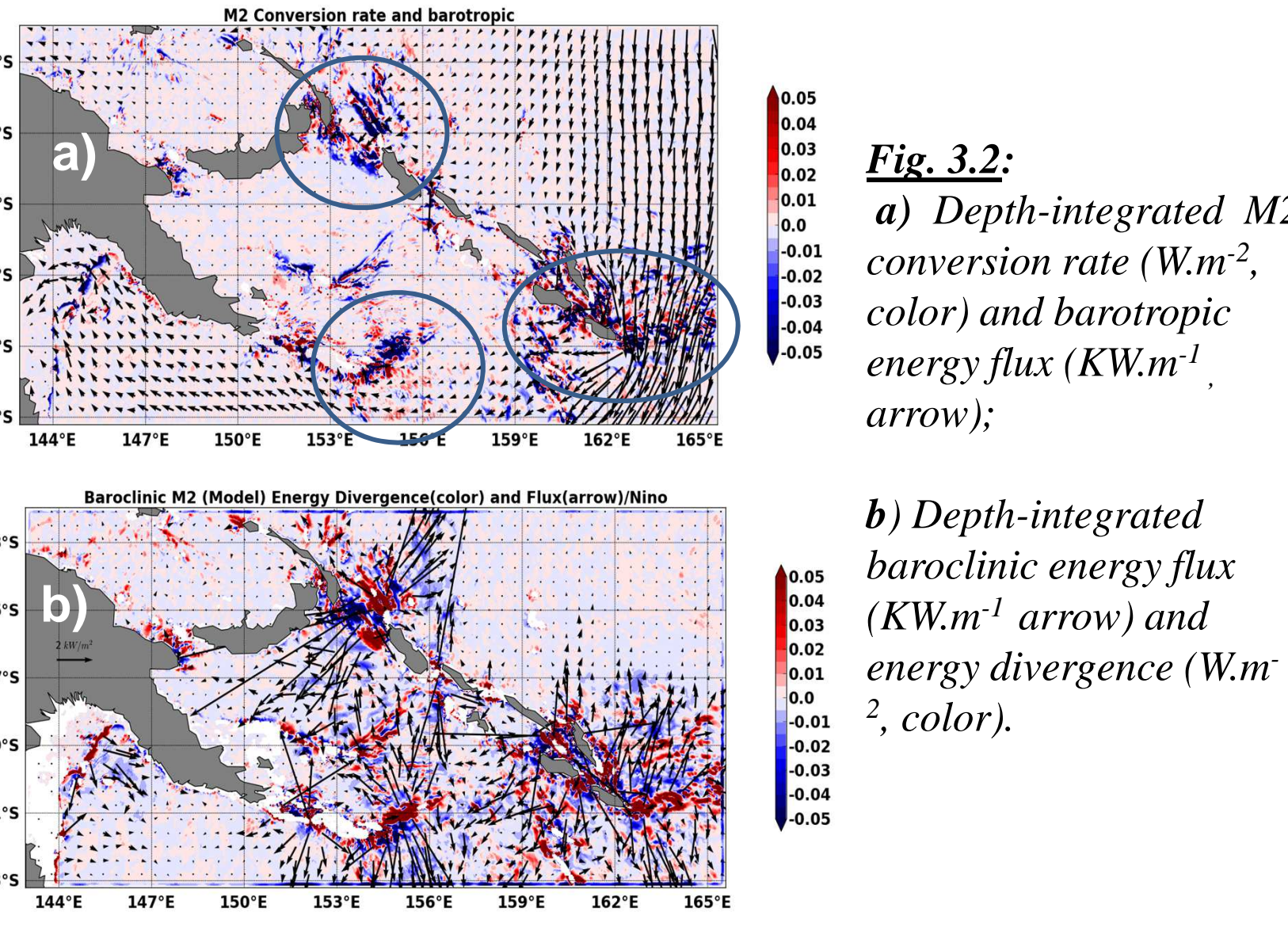


Fig. 3.2: a) Depth-integrated M2 conversion rate ($W.m^{-2}$, color) and barotropic energy flux ($KW.m^{-1}$, arrow); b) Depth-integrated baroclinic energy flux ($KW.m^{-1}$ arrow) and energy divergence ($W.m^{-2}$, color).

Influence of ENSO variability

- **El Niño:** Low EKE → low incoherent tides
Stratification in the upper layers → Unstructured internal tides
- **La Niña:** High EKE → large incoherent tides
Deep stratification → Structured internal tides

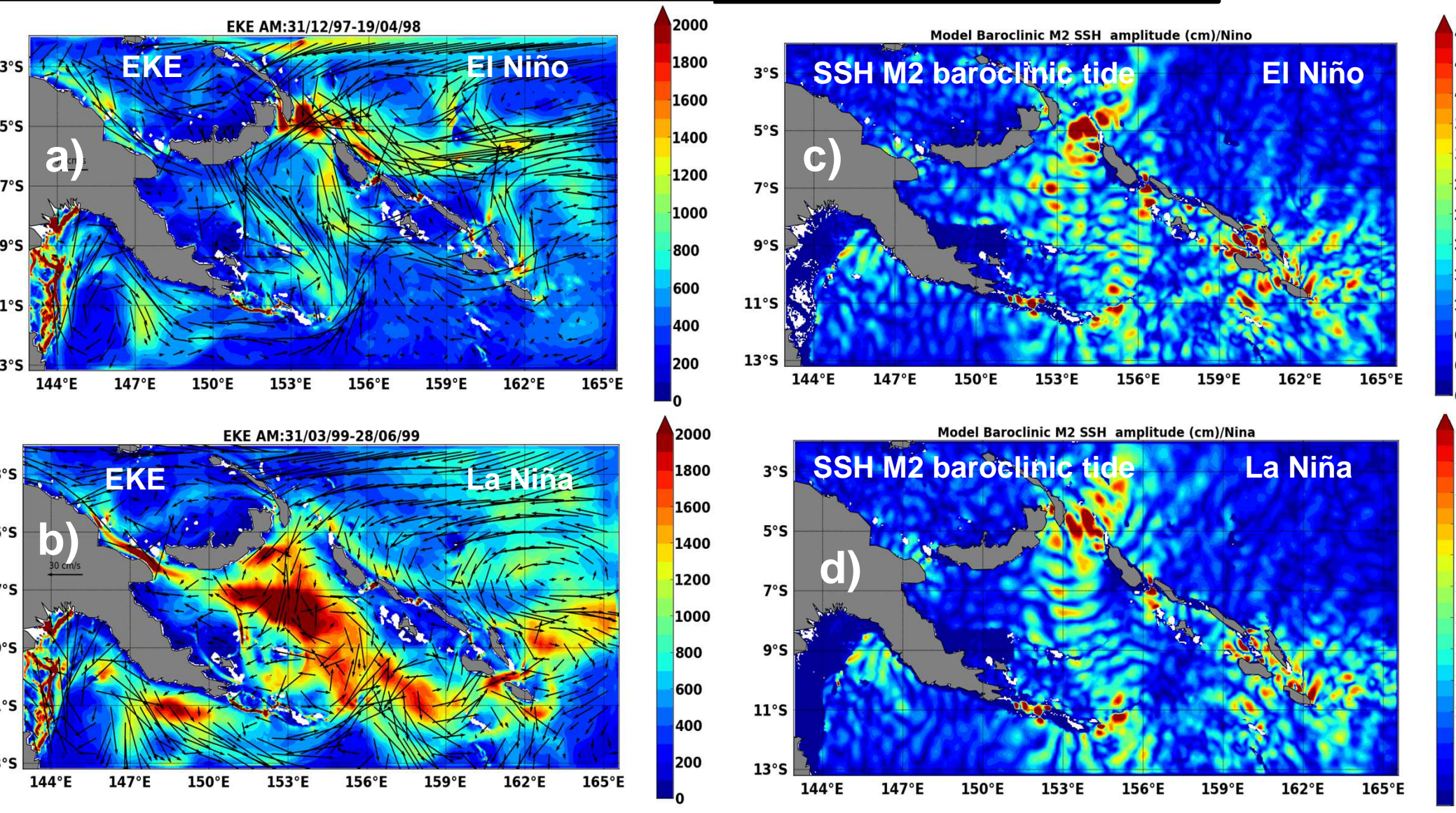


Fig. 3.3: High frequency EKE during a) El Niño and b) La Niña. SSH signature of the M2 baroclinic tide during c) El Niño and d) La Niña. e) Brunt Väisälä profiles for the mean modeled conditions (blue), El Niño conditions (green), La Niña conditions (red). The CARS climatology is in cyan.

Evidence of diapycnal mixing due to tides

- UTW salinity maximum erosion in the presence of tides

Fig. 3.4: Mean salinity difference (1998-1999) between R36 (no tides) and R36T (with tides) for a) Upper thermocline waters (100-250m) and b) Surface Waters (0-100m).

4. Cal/val experiment in New Caledonia

We propose New Caledonia for a cal/val in situ experiment for the SWOT fast sampling phase.

The main motivations are :

- it is a region of strong mesoscale activity (Fig. 4.2)
- it is a region of strong internal tides (Fig. 4.2)
- it has been actively studied for the validation of Saral/AltiKa (Durand et al. 2017)
- the IRD center in New Caledonia is an appropriate basis for *in situ* experiments



Fig. 4.1: SWOT track over New Caledonia during 1-day orbit

The strategy for a cal/val experiment still needs to be defined from the ongoing analysis of historical in situ observations (SADCP, gliders, thermosalinographs,...) in the region.

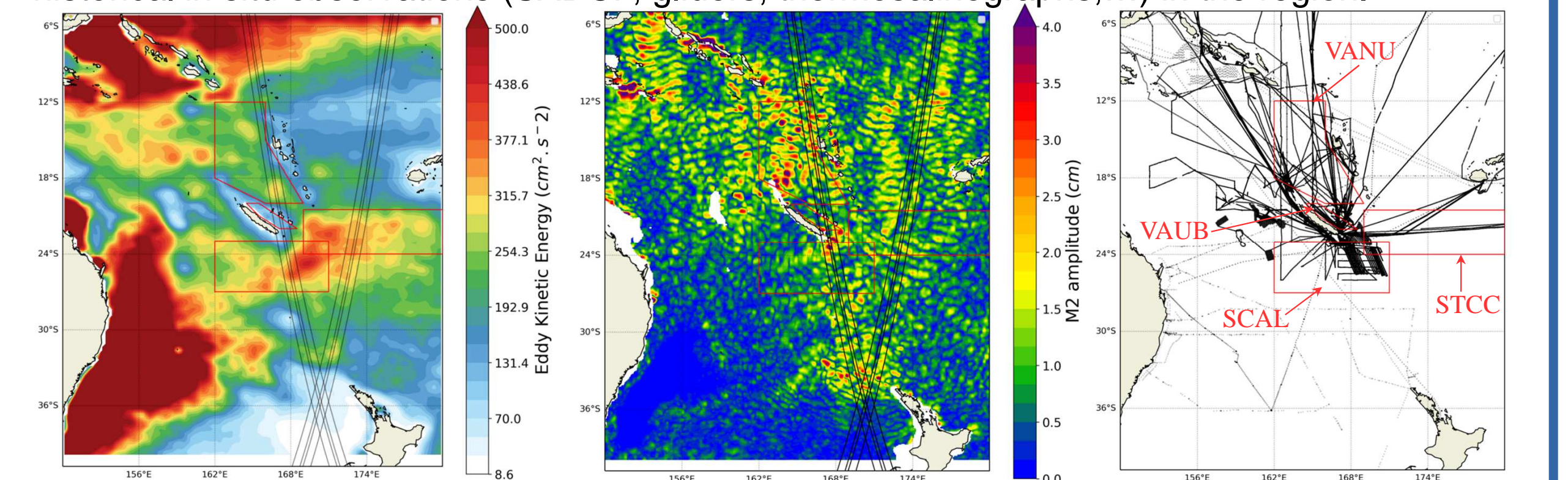


Fig. 4.2: Horizontal distribution from EKE (AVISO), M2 internal tides amplitude (Ray and Zaron 2016) and S-ADCP historical observations in the SouthWest Tropical Pacific. SWOT track during 1-day orbit black line.

Structure functions from S-ADCP

Method: Computation of 2nd-order structure function $D2(r)$ from observed S-ADCP longitudinal () and transverse (⊥) velocities separated by distance r (Balwada et al. 2016)

$$D2(r) = \langle [u(x) - u(x+r)]^2 \rangle$$

• A Helmholtz decomposition is possible if rotational (ψ) and divergent (ϕ) are uncorrelated and the flow is isotropic (Lindborg, 2015):

$$D2_{\psi}(r) = D2_{\psi}(r) + \int_0^r \frac{D2_{\psi}(r') - D2_{\psi}(r')}{r'} dr'$$

$$D2_{\phi}(r) = D2_{\phi}(r) - \int_0^r \frac{D2_{\phi}(r') - D2_{\phi}(r')}{r'} dr'$$

$$D2 = D2_{\psi} + D2_{\phi} = D2_{\psi} + D2_{\phi}$$

• 2nd-order structure function $D2$ is related to classic KE spectrum E and power laws (Lindborg, 2007):

Power law: $E \sim k^{\alpha}$, $D2 \sim r^{-\alpha-1}$

QG: $E \sim k^{-3}$, $D2 \sim r^{-2}$

SQG: $E \sim k^{-2}$, $D2 \sim r^{-1}$

Kolmogorov: $E \sim k^{-5/3}$, $D2 \sim r^{-2/3}$

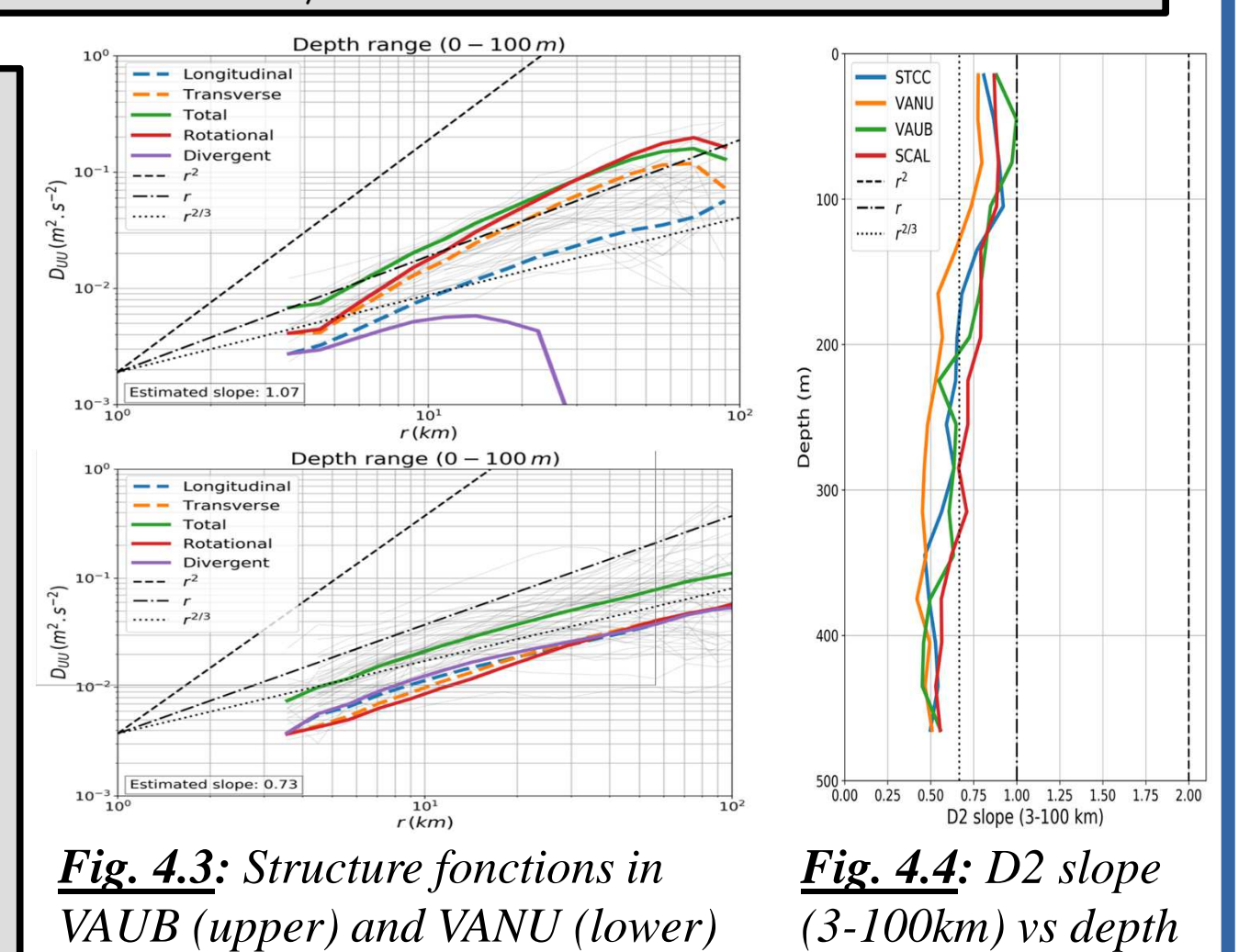


Fig. 4.3: Structure functions in VAUB (upper) and VANU (lower)

In regions of strong mesoscale activities :

- predominance of rotational motions
- sharp transition from SQG (0-100m) to Kolmogorov (below 200m)

→ Other data were analyzed :

- Amplitude of M2 internal tides from isopycnal displacements (gliders)
- surface temperature/salinity from thermosalinographs to estimate scales of the buoyancy
- Sentinel-3 data for SSH spectra

References:

Balwada et al. (2016). Scale-Dependent Distribution of Kinetic Energy from Surface Drifters in the Gulf of Mexico. Geophys. Res. Lett. 43.
Djath et al. (2014). Multiscale analysis of dynamics from high resolution realistic model of the Solomon Sea. J. Geophys. Res. Oceans 119.
Durand et al. (2017). The East Caledonian Current: A Case Example for the Intercomparison between AltiKa and In Situ Measurements in a Boundary Current. Marine Geodesy 40.
Ganachaud et al. (2014). The SouthWest Pacific Ocean circulation and climate experiment (SPICE). J. Geophys. Res. Oceans.
Lindborg (2007). Horizontal Wavenumber Spectra of Vertical Vorticity and Horizontal Divergence in the Upper Troposphere and Lower Stratosphere. J. Atmos. Sci. 64.
Lindborg (2015). A Helmholtz decomposition of structure functions and spectra calculated from aircraft data. J. Fluid Mech. 762.
Ray and Zaron (2016). M2 Internal Tides and Their Observed Wavenumber Spectra from Satellite Altimetry. J. Phys. Oceanogr. 46.
Sérazin et al. Scale-dependent analysis of in situ and altimetric observations in the mesoscale to submesoscale range around New Caledonia, to be submitted
Tchilibou et al. (2018). Spectral signatures of the tropical Pacific dynamics from model and altimetry. Ocean Sci., 14, 1283-1301.
tchilibou et al., Internal tides in the Solomon Sea : Characteristics and impacts, to be submitted
Xu and Fu (2012). The Effects of Altimeter Instrument Noise on the Estimation of the Wavenumber Spectrum of Sea Surface Height. J. Phys. Oceanogr. 42.

